

Estimation of the Wigner distribution of single-mode Gaussian states: A comparative studyChandan Kumar^{1,*} and Arvind^{1,2,†}¹*Department of Physical Sciences, Indian Institute of Science Education and Research Mohali, Sector 81 SAS Nagar, Punjab 140306, India*²*Punjabi University Patiala, Punjab 147002, India* (Received 1 October 2021; revised 5 March 2022; accepted 21 March 2022; published 12 April 2022)

In this work, we consider the estimation of single-mode Gaussian states using four different measurement schemes, namely, (1) homodyne measurement, (2) heterodyne measurement, (3) sequential measurement scheme, and (4) the Arthurs-Kelly measurement scheme, with a view to compare their relative performance. To this end, we work in the phase space formalism, specifically at the covariance matrix level, which provides an elegant and intuitive way to explicitly carry out the involved calculations. We show that the optimal performance of the Arthurs-Kelly and sequential measurement schemes is equal to the heterodyne measurement. While the heterodyne measurement outperforms the homodyne measurement in the mean estimation of squeezed state ensembles, the homodyne measurement outperforms the heterodyne measurement for variance estimation of squeezed state ensembles up to a certain range of the squeezing parameter. We then modify the Hamiltonian in the Arthurs-Kelly measurement scheme, such that the two meters can have correlations and show that the optimal performance is achieved when the meters are uncorrelated. We expect that these results will be useful in various quantum information and quantum communication protocols.

DOI: [10.1103/PhysRevA.105.042419](https://doi.org/10.1103/PhysRevA.105.042419)**I. INTRODUCTION**

Reconstruction of quantum states by performing measurements on an ensemble of systems prepared in identical but unknown states is known as quantum state estimation (QSE) or quantum state tomography (QST) [1–3]. QSE is important in quantum mechanics and quantum information processing, and finding schemes for its efficient execution is an active area of research [4–6]. Ideal QSE requires infinite copies of a quantum system, which is impractical in the real world. Usually an experimentalist is provided with a fixed number of identically prepared systems, and thus one would like to know the advantages and limitations of various measurement schemes and select the best scheme as per the requirements. We consider several different measurement schemes that can be employed for the QSE of continuous variable (CV) systems.

Homodyne measurement is one of the most widely employed measurement schemes in CV systems, which measures either the \hat{q} quadrature or the \hat{p} quadrature or any other phase-rotated quadrature operator [7–10]. It has been shown that various quasiprobability distributions such as Glauber-Sudarshan distribution, Wigner distribution, and Husimi distribution [11] can be estimated using measurements of the rotated quadrature operators and has also been demonstrated experimentally [12]. One can also think of sequential measurement (SM) of a pair of conjugate observables in CV systems, where the observables are measured one after another [13–15]. The sequential measurement of two noncommuting observables has been employed to reconstruct the

Moyal M function, which is the Fourier transform of the Wigner function [14]. Arthurs and Kelly, in a unique effort, extended the von Neumann measurement scheme to the joint measurement of two noncommuting observables [16]. In this joint measurement the consequence of noncommutativity is the introduction of additional minimum noise in the outcomes of both observables. Similarly, a heterodyne measurement, which is equivalent to an eight-port measurement (double-homodyne), can be employed for the joint measurement of two noncommuting observables [17–28]. For the heterodyne measurement, the vacuum noise is added in both noncommuting observables, and unlike in the Arthurs-Kelly measurement scheme this cannot be distributed among the observables at will. It has been shown that the heterodyne measurement can do a better estimation of the first- and the second-order moments of the quadrature operators of Gaussian and non-Gaussian states compared to the homodyne measurement [29–31]. The superiority of localized phase space sampling with unbalanced homodyne measurement [32] compared to delocalized heterodyne measurement has also been shown [33].

In this article, we provide a comparative study of the state estimation efficiency of different measurement schemes including homodyne measurement, heterodyne measurement, sequential measurement scheme, and the Arthurs-Kelly measurement scheme. To this end, we consider an ensemble of N identically prepared single-mode Gaussian states. Gaussian states are defined as states with a Gaussian Wigner distribution function, and we need to estimate the mean and the covariance matrix to completely reconstruct such states. We further assume that the Gaussian states are squeezed in either the \hat{q} or the \hat{p} quadrature. Such states have been employed in squeezed state CV quantum key distribution (QKD) protocols [34–36] and are easier to estimate.

*chandan.quantum@gmail.com

†arvind@iisermohali.ac.in

We provide analytical expressions of the estimation efficiency of the mean and the variance of an ensemble of N identically prepared Gaussian states. We show that the optimal performance of the Arthurs-Kelly and sequential measurement schemes is equal to the heterodyne measurement. For mean estimation, the heterodyne measurement outperforms the homodyne measurement for a squeezed coherent state ensemble, but for variance estimation, the homodyne measurement outperforms the heterodyne measurement for a certain squeezing parameter range. We also explore the effect of environmental interactions and imperfect detectors on the performance of heterodyne and homodyne measurements. It turns out that the homodyne and heterodyne measurements become less precise as the interaction time increases. The results also show that the heterodyne measurement is more robust for the distance measure d_1 at all interaction time, while for the distance measure d_2 , the heterodyne measurement is more robust beyond a certain interaction time. Then we proceed to a modified Hamiltonian [37,38] in the Arthurs-Kelly measurement scheme that can entangle the two meters. Here the results show that the optimal performance of the scheme can be obtained only when the meters are uncorrelated. Since the Hamiltonians involved in the sequential and the Arthurs-Kelly measurement schemes are quadratic expressions in quadrature operators, the corresponding symplectic transformations acting on the quadrature operators or the phase space variables belong to the real symplectic group $\text{Sp}(4, \mathcal{R})$ and $\text{Sp}(6, \mathcal{R})$ [39], respectively. We exploit this fact and explicitly work in phase space for calculational simplicity.

We expect that these techniques along with the results obtained in this work will be useful in undertaking various studies in different quantum information and quantum communication protocols [40,41]. For instance, the sequential measurement scheme considered in the current work can be exploited to investigate the interplay between the quality of estimation of the quadratures via homodyne (phase-sensitive) measurement and the disturbance in the reduced state of the system. This analysis will complement earlier works, where the quality of estimation of a coherent state via phase-insensitive measurements and the disturbance in the postmeasurement state has been examined [42,43]. This study will also be useful in the reconsideration of an experimental study where measurements of the leakage modes are performed to retrieve the information encoded in the Gaussian state [44].

This article is organized as follows. In Sec. II A we present the basic formalism of the CV system, while in Sec. II B we introduce various measurement schemes and obtain the variance of probability distributions corresponding to different quadrature measurements. In Sec. III we analyze the performance of various measurement schemes in the mean and the variance estimation. In Sec. IV we consider the Arthurs-Kelly measurement scheme with a modified interaction Hamiltonian. Finally, in Sec. V we provide concluding remarks and discuss future prospects.

II. BACKGROUND

In this section, we introduce the formalism of an n -mode CV system and describe various measurement schemes.

A. Description of an n -mode CV system

An n -mode continuous variable quantum system can arise in different contexts, ranging from n -physical harmonic oscillators to n -modes of the electromagnetic field or of the lattice vibrations. Although the description here is general, the physical system that we have in mind is n -modes of the electromagnetic field.

An n -mode quantum CV system is described by n pairs of Hermitian quadrature operators, which can be collected in a vector form as follows [40,41,45,46]:

$$\hat{\xi} = (\hat{\xi}_i) = (\hat{q}_1, \hat{p}_1, \dots, \hat{q}_n, \hat{p}_n)^T, \quad i = 1, 2, \dots, 2n. \quad (1)$$

The canonical commutation relations can be written compactly as (with $\hbar = 1$)

$$[\hat{\xi}_i, \hat{\xi}_j] = i\Omega_{ij}, \quad (i, j = 1, 2, \dots, 2n), \quad (2)$$

where Ω is the symplectic form given by

$$\Omega = \bigoplus_{k=1}^n \omega = \begin{pmatrix} \omega & & \\ & \ddots & \\ & & \omega \end{pmatrix}, \quad \omega = \begin{pmatrix} 0 & 1 \\ -1 & 0 \end{pmatrix}. \quad (3)$$

The Hilbert space of the n -mode system is spanned by the product basis vector $|n_1 \dots n_i \dots n_n\rangle$ with $\{n_1, \dots, n_i, \dots, n_n = 0, 1, \dots, \infty\}$, where the number n_i corresponds to the photon number in the i th mode. The quantum states of this system are represented via density operators in this Hilbert space. The density operator $\hat{\rho}$ is a Hermitian, nonnegative and trace-one class operator.

We can alternatively describe an n -mode system in a $2n$ -dimensional phase space. The Wigner distribution for a quantum system with density operator $\hat{\rho}$ can be written as [47]

$$W(\xi) = (2\pi)^{-n} \int d^n q' \left\langle q - \frac{1}{2}q' | \hat{\rho} | q + \frac{1}{2}q' \right\rangle \exp(iq' \cdot p), \quad (4)$$

where $q = (q_1, q_2, \dots, q_n)^T$, $p = (p_1, p_2, \dots, p_n)^T$, and $\xi = (q_1, p_1, \dots, q_n, p_n)^T$. Thus, $W(\xi)$ is a function of $2n$ real phase space variables for an n -mode quantum system. The first-order moments (sometimes called displacement or mean) vector is given as

$$\bar{\xi} = \text{Tr}[\hat{\rho}\hat{\xi}]. \quad (5)$$

Similarly, the second-order moments, which are best represented in the form of a $2n \times 2n$, real symmetric matrix, called the covariance matrix is given as

$$V = (V_{ij}) = \frac{1}{2} \langle \{\Delta\hat{\xi}_i, \Delta\hat{\xi}_j\} \rangle, \quad (6)$$

where $\Delta\hat{\xi}_i = \hat{\xi}_i - \langle \hat{\xi}_i \rangle$, and $\{, \}$ denotes an anticommutator. The uncertainty principle obeyed by all quantum states can be expressed easily in terms of covariance matrix as

$$V + \frac{i}{2}\Omega \geq 0. \quad (7)$$

The class of Gaussian states, which is the focus of our work, is defined as a set of states with a Gaussian Wigner distribution given as [41]

$$W(\xi) = \frac{\exp[-(1/2)(\xi - \bar{\xi})^T V^{-1}(\xi - \bar{\xi})]}{(2\pi)^n \sqrt{\det V}}, \quad (8)$$

where V is the covariance matrix and $\bar{\xi}$ denotes the displacement of the Gaussian state.

As an example, the covariance matrix of single-mode vacuum state $\hat{\rho} = |0\rangle\langle 0|$ is written as

$$V_{|0\rangle} = \frac{1}{2} \begin{pmatrix} \langle\{\Delta q, \Delta q\}\rangle & \langle\{\Delta q, \Delta p\}\rangle \\ \langle\{\Delta p, \Delta q\}\rangle & \langle\{\Delta p, \Delta p\}\rangle \end{pmatrix} = \frac{1}{2} \begin{pmatrix} 1 & 0 \\ 0 & 1 \end{pmatrix}. \quad (9)$$

Similarly, for a single-mode thermal state,

$$\hat{\rho} = \sum_{n=0}^{\infty} \frac{\langle n \rangle^n}{(1 + \langle n \rangle)^{n+1}} |n\rangle\langle n|, \quad (10)$$

where $\langle n \rangle = 1/[\exp(\omega/k_B T) - 1]$ is the average number of photons in the thermal state, the covariance matrix is given by

$$V_{\text{th}} = \frac{1}{2} \begin{pmatrix} 2\langle n \rangle + 1 & 0 \\ 0 & 2\langle n \rangle + 1 \end{pmatrix}. \quad (11)$$

We note that the vacuum state and the thermal state are prominent examples of Gaussian states.

Symplectic transformation

The linear homogeneous transformations described by real $2n \times 2n$ matrices S act on the quadrature operators as $\hat{\xi}_i \rightarrow \hat{\xi}'_i = S_{ij}\hat{\xi}_j$. These matrices S form a noncompact group called the symplectic group $\text{Sp}(2n, \mathcal{R})$ in $2n$ dimensions if they satisfy the following condition in order to preserve the canonical commutation relation Eq. (2):

$$\text{Sp}(2n, \mathcal{R}) = \{S \mid S\Omega S^T = \Omega\}. \quad (12)$$

The symplectic transformation S acts on the Hilbert space of the system via its infinite dimensional unitary representation $\mathcal{U}(S)$, also known as a metaplectic representation. The elements of this metaplectic representation are generated by quadratic Hamiltonians. Under a symplectic transformation S , the density operator, mean, and covariance matrix for any quantum state transform as

$$\rho \rightarrow \mathcal{U}(S)\rho\mathcal{U}(S)^\dagger \Rightarrow \bar{\xi} \rightarrow S\bar{\xi}, \quad V \rightarrow SVS^T. \quad (13)$$

In this paper we will be focusing on single-mode Gaussian states with a diagonal covariance matrix with displacement vector $\bar{\xi}$ and covariance matrix V given by

$$\bar{\xi} = \begin{pmatrix} q_0 \\ p_0 \end{pmatrix}, \quad V = \begin{pmatrix} (\Delta q)^2 & 0 \\ 0 & (\Delta p)^2 \end{pmatrix}, \quad (14)$$

where $q_0 = \langle \hat{q} \rangle$, $p_0 = \langle \hat{p} \rangle$, $(\Delta q)^2 = \langle \hat{q}^2 \rangle - (\langle \hat{q} \rangle)^2$, and $(\Delta p)^2 = \langle \hat{p}^2 \rangle - (\langle \hat{p} \rangle)^2$. The corresponding Gaussian Wigner distribution as per Eq. (8) is given as

$$W(q, p) = \frac{1}{2\pi\Delta q\Delta p} \exp \left[-\frac{(q - q_0)^2}{2(\Delta q)^2} - \frac{(p - p_0)^2}{2(\Delta p)^2} \right]. \quad (15)$$

For analysis purposes in the later sections, we shall use the explicit form of the covariance matrix for a squeezed coherent thermal state corresponding to temperature T of a single-mode system with frequency ω , which is

given by

$$V = S(r)V_{\text{th}}S(r)^T = \frac{1}{2} \begin{pmatrix} (2\langle n \rangle + 1)e^{-2r} & 0 \\ 0 & (2\langle n \rangle + 1)e^{2r} \end{pmatrix}, \quad (16)$$

where $S(r)$ is the single-mode squeezing transformation given by

$$S(r) = \begin{pmatrix} e^{-r} & 0 \\ 0 & e^r \end{pmatrix}. \quad (17)$$

This is the family of states that we will estimate using different techniques in this paper.

B. Measurement schemes

In this section, various measurement schemes for state estimation which we intend to compare are described. A Gaussian model for measurements is assumed where any measured quantity when repeatedly measured is fitted to a Gaussian in the sense that we infer the mean and variance from the distribution. The variance of the probability distribution signifies the accuracy of the corresponding measurement scheme. While the analysis in the following sections neglects interactions with the environment and considers perfect detectors, interactions with the environment and imperfect detectors have been considered in Sec. III D.

1. Homodyne measurement

In homodyne measurement, we perform the measurement of either the quadrature \hat{q} or the quadrature \hat{p} on the system [7–10]. The probability distribution function $P(q)$ of obtaining the outcome q corresponding to the measurement of the \hat{q} quadrature on the state given in Eq. (14) can be evaluated as

$$P(q) = \int W(q, p) dp = \frac{1}{\sqrt{2\pi(\Delta q)^2}} \exp \left[-\frac{(q - q_0)^2}{2(\Delta q)^2} \right]. \quad (18)$$

Therefore, the corresponding variance for the \hat{q} quadrature measurement is

$$V^{\text{Hom}}(\hat{q}) = (\Delta q)^2. \quad (19)$$

This variance is for an infinite ensemble limit. If we have to estimate the \hat{p} quadrature, we need to use a distinct ensemble that is prepared in the same way and that has not undergone the \hat{q} quadrature measurement. The probability distribution function $P(p)$ of obtaining the outcome p corresponding to the measurement of the \hat{p} quadrature on the state (14) can be evaluated as

$$P(p) = \int W(q, p) dq = \frac{1}{\sqrt{2\pi(\Delta p)^2}} \exp \left[-\frac{(p - p_0)^2}{2(\Delta p)^2} \right]. \quad (20)$$

Therefore, the corresponding variance for the \hat{p} quadrature measurement is

$$V^{\text{Hom}}(\hat{p}) = (\Delta p)^2. \quad (21)$$

2. Heterodyne measurement

In heterodyne measurement, we jointly measure the \hat{q} quadrature and the \hat{p} quadrature on the system [17–28]. Since

the heterodyne measurement corresponds to the projection onto coherent state basis $E_\alpha = (2\pi)^{-1}|\alpha\rangle\langle\alpha|$, the probability of obtaining the outcomes q and p on the joint measurement of the q and p quadratures on a system with density operator ρ can be written as

$$P(q, p) = \frac{1}{2\pi} \text{Tr}[\hat{\rho}|\alpha\rangle\langle\alpha|]. \quad (22)$$

For simplicity, we move to the phase space and evaluate the trace in the Wigner function description as follows:

$$P(q, p) = \int_{\mathcal{R}^2} dq dp W_\rho(q, p) W_{|\alpha\rangle}(q, p). \quad (23)$$

The probability distribution function can then be calculated and is given by

$$P(q, p) = \frac{\exp\left[-\frac{(q-q_0)^2}{1+2(\Delta q)^2} - \frac{(p-p_0)^2}{1+2(\Delta p)^2}\right]}{\pi\sqrt{[1+2(\Delta q)^2][1+2(\Delta p)^2]}}. \quad (24)$$

Therefore, the corresponding variance of the marginals $P(q)$ and $P(p)$ of the probability distribution $P(q, p)$ is

$$V^{\text{Het}}(\hat{q}) = \frac{1}{2} + (\Delta q)^2 \quad \text{and} \quad V^{\text{Het}}(\hat{p}) = \frac{1}{2} + (\Delta p)^2. \quad (25)$$

We note that the vacuum noise (equal to $1/2$) is added to the variance of both marginals $P(q)$ and $P(p)$ of the probability distribution $P(q, p)$.

3. Sequential measurement scheme

In the sequential measurement scheme, the measurement of one quadrature is followed by the measurement of its conjugate quadrature [13–15]. To carry out the first measurement, we use the von Neumann measurement model, where we couple the system with a meter. The state of the system is inferred through the readings of the meter. The second measurement, i.e., the measurement of the conjugate observable, is a homodyne measurement. To remove the biasedness in the order of the measurements, we divide the ensemble in two halves [15]. On the first half, we measure the \hat{Q} quadrature of the meter weakly, which renders information about the \hat{q} quadrature of the system. This weak measurement disturbs the state a little and does not lead to the complete collapse of the wave function, and therefore, the state can be reused for measurement. This is followed by a homodyne measurement of the \hat{p} quadrature on the system, as shown in Fig. 1. Similarly, on the second half, the weak measurement of \hat{Q} quadrature of the meter renders information about the \hat{p} quadrature of the system, which is followed by a homodyne measurement of the \hat{q} quadrature of the system. We now describe the scheme in detail. While the system is represented by the quadrature operators \hat{q} and \hat{p} , we consider the apparatus also to be a one-mode CV system representing a meter with quadrature operators \hat{Q}_1 and \hat{P}_1 . The corresponding phase space is four-dimensional and can be represented by four variables, which can be arranged in a column vector form as $\xi = (q, p, Q_1, P_1)^T$. We assume that the system is in a squeezed coherent thermal state and the meter is in a squeezed vacuum state, and thus they satisfy the following uncertainty relations:

$$\Delta q \Delta p \geq 1/2, \quad \Delta Q_1 \Delta P_1 = 1/2. \quad (26)$$

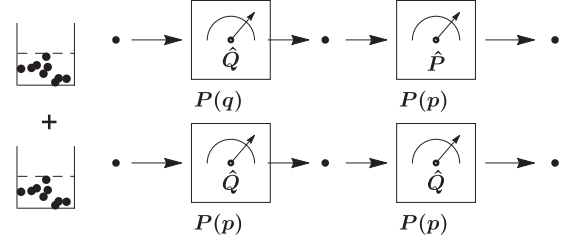


FIG. 1. Schematic representation of the sequential measurement scheme. The whole ensemble is divided in two halves. On the first half, the sequential measurement of the \hat{Q} quadrature of the meter, which renders information about the \hat{q} quadrature of the system, is followed by a homodyne measurement of the \hat{p} quadrature of the system. Similarly, on the second half, the sequential measurement of the \hat{Q} quadrature of the meter, which renders information about the \hat{p} quadrature of the system, is followed by a homodyne measurement of the \hat{q} quadrature of the system.

Since the system and the meter are in Gaussian states, the system-meter state can be specified by the following displacement vector and covariance matrix:

$$\begin{aligned} \bar{\xi} &= \begin{pmatrix} \langle \hat{q} \rangle = q_0 \\ \langle \hat{p} \rangle = p_0 \\ \langle \hat{Q}_1 \rangle = 0 \\ \langle \hat{P}_1 \rangle = 0 \end{pmatrix}, \\ V &= \begin{pmatrix} (\Delta q)^2 & 0 & 0 & 0 \\ 0 & (\Delta p)^2 & 0 & 0 \\ 0 & 0 & (\Delta Q_1)^2 & 0 \\ 0 & 0 & 0 & (\Delta P_1)^2 \end{pmatrix}. \end{aligned} \quad (27)$$

Now we consider the interaction Hamiltonian of the form

$$\hat{H}(t) = \delta(t - t_1) \hat{q} \hat{P}_1, \quad (28)$$

which entangles the system and the meter. The unitary operator acting on the joint system-meter Hilbert space for $t > t_1$ is given by

$$\mathcal{U}(\hat{H}(t)) = e^{-i \int \hat{H}(t) dt} = e^{-i \hat{q} \hat{P}_1}. \quad (29)$$

The corresponding symplectic transformation acting on the quadrature operators $\hat{\xi} = (\hat{q}, \hat{p}, \hat{Q}_1, \hat{P}_1)^T$ is given by (see Appendix A)

$$S = \begin{pmatrix} 1 & 0 & 0 & 0 \\ 0 & 1 & 0 & -1 \\ 1 & 0 & 1 & 0 \\ 0 & 0 & 0 & 1 \end{pmatrix}. \quad (30)$$

The above symplectic transformation is an element of the real symplectic group $\text{Sp}(4, \mathcal{R})$ and satisfies the symplectic condition (12). As a result of the above transformation, the final displacement vector and covariance matrix V (27) can be written as follows according to Eq. (13):

$$\bar{\xi}' = \begin{pmatrix} \langle \hat{q} \rangle = q_0 \\ \langle \hat{p} \rangle = p_0 \\ \langle \hat{Q}_1 \rangle = q_0 \\ \langle \hat{P}_1 \rangle = 0 \end{pmatrix} \quad (31)$$

and

$$V' = \begin{pmatrix} (\Delta q)^2 & 0 & (\Delta q)^2 & 0 \\ 0 & (\Delta p)^2 + (\Delta P_1)^2 & 0 & -(\Delta P_1)^2 \\ (\Delta q)^2 & 0 & (\Delta q)^2 + (\Delta Q_1)^2 & 0 \\ 0 & -(\Delta P_1)^2 & 0 & (\Delta P_1)^2 \end{pmatrix}. \quad (32)$$

One can easily find the transformed Wigner distribution of the system meter using Eq. (8), which is specified by the displacement vector (31) and the covariance matrix (32). The Wigner distribution of the reduced state of the meter can be evaluated by integrating the system-meter Wigner distribution over the system variables q and p . The displacement vector and the covariance matrix of the reduced state can be readily evaluated using the Wigner function of the reduced state. An alternative to this approach is to work at the covariance matrix level. The displacement vector and the covariance matrix of the reduced state of the meter can be obtained by ignoring the matrix elements corresponding to the system mode. This can be easily seen through the Wigner characteristic function of a Gaussian state [46,48]. Thus, the displacement vector and the covariance matrix of the reduced state of the meter are

$$\overline{\xi}'_M = \left(\begin{array}{l} \langle \hat{Q}_1 \rangle = q_0 \\ \langle \hat{P}_1 \rangle = 0 \end{array} \right), \quad V'_M = \begin{pmatrix} (\Delta q)^2 + (\Delta Q_1)^2 & 0 \\ 0 & (\Delta P_1)^2 \end{pmatrix}. \quad (33)$$

The corresponding Wigner function for the reduced state of the meter can be written using Eq. (8) as

$$W(Q_1, P_1) = \frac{1}{2\pi \Delta P_1 \sqrt{(\Delta q)^2 + (\Delta Q_1)^2}} \times \exp \left[-\frac{(Q_1 - q_0)^2}{2((\Delta q)^2 + (\Delta Q_1)^2)} - \frac{P_1^2}{2(\Delta P_1)^2} \right]. \quad (34)$$

The probability density to obtain the outcome Q_1 after a measurement of the \hat{Q}_1 quadrature on the meter is

$$P(Q_1) = \frac{1}{\sqrt{2\pi[(\Delta q)^2 + (\Delta Q_1)^2]}} \times \exp \left\{ -\frac{(Q_1 - q_0)^2}{2[(\Delta q)^2 + (\Delta Q_1)^2]} \right\}. \quad (35)$$

Clearly the variance of the probability distribution is

$$V_1^{\text{SM}}(\hat{q}) = (\Delta q)^2 + (\Delta Q_1)^2, \quad (36)$$

which we could have directly written from Eq. (32) as the element corresponding to the variance of Q_1 . Similarly, the displacement vector and the covariance matrix of the reduced state of the system are given by

$$\overline{\xi}'_S = \left(\begin{array}{l} \langle \hat{Q}_1 \rangle = q_0 \\ \langle \hat{P}_1 \rangle = p_0 \end{array} \right), \quad V'_S = \begin{pmatrix} (\Delta q)^2 & 0 \\ 0 & (\Delta p)^2 + (\Delta P_1)^2 \end{pmatrix}. \quad (37)$$

According to Eq. (36), more precise information about the \hat{q} quadrature of the system can be obtained by decreasing the value of ΔQ_1 , which leads to an increment in ΔP_1 . Consequently, the reduced state of the system (37) gets more disturbed. Hence the sequential measurement scheme enables us to study the interplay between the quality of estimation of the quadratures via homodyne (phase-sensitive) measurement

and the disturbance in the reduced state of the system. The trade-off between the quality of estimation of coherent state via phase-insensitive measurements and the disturbance in the postmeasurement state has been studied in Refs. [42,43].

The variance of the probability distribution corresponding to the homodyne measurement of the \hat{p} quadrature on the reduced state of the system (37) is given by

$$V_1^{\text{SM}}(\hat{p}) = (\Delta p)^2 + (\Delta P_1)^2. \quad (38)$$

We now discuss the weak measurement of the \hat{p} quadrature followed by a homodyne measurement of the \hat{q} quadrature. We again consider the initial state of the joint system-meter state being represented by the displacement vector and the covariance matrix as given in Eq. (27). We consider the interaction Hamiltonian of the form

$$\hat{H}(t) = \delta(t - t_1) \hat{p} \hat{Q}_1, \quad (39)$$

which is the generator of the following symplectic transformation:

$$S = \begin{pmatrix} 1 & 0 & 0 & 1 \\ 0 & 1 & 0 & 0 \\ 0 & 1 & 1 & 0 \\ 0 & 0 & 0 & 1 \end{pmatrix}. \quad (40)$$

The above symplectic transformation is also an element of the real symplectic group $\text{Sp}(4, \mathcal{R})$ and satisfies the symplectic condition (12). The final system-meter state after the action of the above symplectic transformation can be specified by the following displacement vector and covariance matrix:

$$\overline{\xi}' = \left(\begin{array}{l} \langle \hat{q} \rangle = q_0 \\ \langle \hat{p} \rangle = p_0 \\ \langle \hat{Q}_1 \rangle = p_0 \\ \langle \hat{P}_1 \rangle = 0 \end{array} \right) \quad (41)$$

and

$$V' = \begin{pmatrix} (\Delta q)^2 + (\Delta P_1)^2 & 0 & 0 & (\Delta P_1)^2 \\ 0 & (\Delta p)^2 & (\Delta p)^2 & 0 \\ 0 & (\Delta p)^2 & (\Delta p)^2 + (\Delta Q_1)^2 & 0 \\ (\Delta P_1)^2 & 0 & 0 & (\Delta P_1)^2 \end{pmatrix}. \quad (42)$$

The displacement vector (41) shows that the mean of the \hat{Q}_1 quadrature for the meter is p_0 . Thus, the measurement of the \hat{Q}_1 quadrature of the meter yields information about the \hat{p} quadrature of the system. We can directly write the variance of the probability distributions corresponding to the sequential measurement of the \hat{Q}_1 quadrature of the meter followed by a homodyne measurement of the \hat{q} quadrature from Eq. (41) as

$$V_2^{\text{SM}}(\hat{p}) = (\Delta q)^2 + (\Delta P_1)^2 \quad \text{and} \\ V_2^{\text{SM}}(\hat{q}) = (\Delta p)^2 + (\Delta Q_1)^2. \quad (43)$$

4. The Arthurs-Kelly measurement scheme

Arthurs-Kelly proposed a scheme by extending the von Neumann model, which enables us to simultaneously measure conjugate quadratures \hat{q} and \hat{p} [16]. To this end, two meters, one for each quadrature measurement, are introduced, as shown in Fig. 2. We represent the system and two meters using three pairs of Hermitian quadrature operators arranged

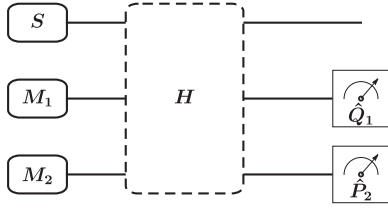


FIG. 2. Schematic representation of the Arthurs-Kelly measurement scheme. The system is labeled by S , and the two meters are labeled by M_1 and M_2 . H represents the interaction Hamiltonian. Measurement of the \hat{Q}_1 quadrature on meter M_1 and measurement of the \hat{P}_2 quadrature on meter M_2 yield information about the \hat{q} quadrature and the \hat{p} quadrature of the system, respectively.

$$\bar{\xi} = \begin{pmatrix} \langle \hat{q} \rangle = q_0 \\ \langle \hat{p} \rangle = p_0 \\ \langle \hat{Q}_1 \rangle = 0 \\ \langle \hat{P}_1 \rangle = 0 \\ \langle \hat{Q}_2 \rangle = 0 \\ \langle \hat{P}_2 \rangle = 0 \end{pmatrix}, \quad V = \begin{pmatrix} \text{System} & & & & & \\ & q & p & & & \\ & (\Delta q)^2 & 0 & & & \\ & 0 & (\Delta p)^2 & & & \\ & 0 & 0 & \text{Meter 1} & & \\ & 0 & 0 & Q_1 & P_1 & \text{Meter 2} \\ & 0 & 0 & (\Delta Q_1)^2 & 0 & Q_2 & P_2 \\ & 0 & 0 & 0 & (\Delta P_1)^2 & 0 & 0 \\ & 0 & 0 & 0 & 0 & (\Delta Q_2)^2 & 0 \\ & 0 & 0 & 0 & 0 & 0 & (\Delta P_2)^2 \end{pmatrix} \begin{matrix} q \\ p \\ Q_1 \\ P_1 \\ Q_2 \\ P_2 \end{matrix}. \quad (45)$$

The interaction Hamiltonian through which we intend to measure both system quadratures by coupling them to different meters is considered to be of the form

$$H = \delta(t - t_1)(\hat{q}\hat{P}_1 - \hat{p}\hat{Q}_2), \quad (46)$$

which entangles the system with both meters. The corresponding symplectic transformation acting on the quadrature operators $\bar{\xi}$ is given by

$$S = \begin{pmatrix} q & p & Q_1 & P_1 & Q_2 & P_2 \\ 1 & 0 & 0 & 0 & -1 & 0 \\ 0 & 1 & 0 & -1 & 0 & 0 \\ 1 & 0 & 1 & 0 & -\frac{1}{2} & 0 \\ 0 & 0 & 0 & 1 & 0 & 0 \\ 0 & 0 & 0 & 0 & 1 & 0 \\ 0 & 1 & 0 & -\frac{1}{2} & 0 & 1 \end{pmatrix} \begin{matrix} q \\ p \\ Q_1 \\ P_1 \\ Q_2 \\ P_2 \end{matrix}. \quad (47)$$

The above symplectic transformation is an element of the real symplectic group $\text{Sp}(6, \mathcal{R})$ and satisfies the symplectic condition (12). The displacement vector and the covariance matrix of the transformed joint system-meters state is explicitly written in Eqs. (B1) and (B2) of Appendix B. The displacement vector and the covariance matrix of the reduced state of the system can be readily written using Eqs. (B1) and (B2) as

$$\bar{\xi}'_S = \begin{pmatrix} \langle \hat{Q}_1 \rangle = q_0 \\ \langle \hat{P}_1 \rangle = p_0 \end{pmatrix},$$

in a column vector as $\bar{\xi} = (\hat{q}, \hat{p}, \hat{Q}_1, \hat{P}_1, \hat{Q}_2, \hat{P}_2)^T$, where (\hat{q}, \hat{p}) corresponds to the system, and (\hat{Q}_1, \hat{P}_1) and (\hat{Q}_2, \hat{P}_2) correspond to the two meters. We assume the system to be in a squeezed coherent thermal state and the meters to be in a squeezed vacuum state, and thus they satisfy the following uncertainty relations:

$$\Delta q \Delta p \geq 1/2, \quad \Delta Q_1 \Delta P_1 = 1/2, \quad \Delta Q_2 \Delta P_2 = 1/2. \quad (44)$$

We analyze our joint system in a six-dimensional phase space represented by six variables, which can be arranged in a column vector form as $\xi = (q, p, Q_1, P_1, Q_2, P_2)^T$. We represent the system-meters state by the displacement vector $\bar{\xi}$ and covariance matrix V as

$$V'_S = \begin{pmatrix} (\Delta q)^2 + (\Delta Q_2)^2 & 0 \\ 0 & (\Delta p)^2 + (\Delta P_1)^2 \end{pmatrix}. \quad (48)$$

Similarly, the displacement vector and the covariance matrix of meter 1 can be written as

$$\bar{\xi}'_{M_1} = \begin{pmatrix} \langle \hat{Q}_1 \rangle = q_0 \\ \langle \hat{P}_1 \rangle = 0 \end{pmatrix}, \quad V'_{M_1} = \begin{pmatrix} (\Delta q)^2 + (\Delta Q_1)^2 + \frac{(\Delta Q_2)^2}{4} & 0 \\ 0 & (\Delta P_1)^2 \end{pmatrix}. \quad (49)$$

Finally, meter 2 is represented by the following displacement vector and covariance matrix:

$$\bar{\xi}'_{M_2} = \begin{pmatrix} \langle \hat{Q}_1 \rangle = 0 \\ \langle \hat{P}_1 \rangle = p_0 \end{pmatrix}, \quad V'_{M_2} = \begin{pmatrix} (\Delta Q_2)^2 & 0 \\ 0 & (\Delta p)^2 + \frac{(\Delta P_1)^2}{4} + (\Delta P_2)^2 \end{pmatrix}. \quad (50)$$

The variance of the probability distribution for the measurement of the \hat{Q}_1 quadrature on meter 1 and \hat{P}_2 quadrature on meter 2 can be directly written from Eq. (B2) as

$$V^{\text{AK}}(\hat{q}) = (\Delta q)^2 + (\Delta Q_1)^2 + \frac{(\Delta Q_2)^2}{4}, \quad V^{\text{AK}}(\hat{p}) = (\Delta p)^2 + \frac{(\Delta P_1)^2}{4} + (\Delta P_2)^2. \quad (51)$$

III. RESULTS

In this section we turn to the examination of the performance of measurement schemes described in Sec. II in the

estimation of the Wigner distribution of an ensemble with a fixed number N of identically prepared Gaussian states. To this end, we define a distance measure d_1 for the accuracy estimation of the mean of the Gaussian state as

$$d_1 = \langle (q^A - q^M)^2 \rangle + \langle (p^A - p^M)^2 \rangle, \quad (52)$$

where q^A and p^A are the actual values of the mean of the \hat{q} and \hat{p} quadratures of the Gaussian state and are thus fixed, whereas q^M and p^M are the measured values of the \hat{q} and \hat{p} quadratures of the Gaussian state. While q^A and p^A are the same for each copy of the ensemble, the values q^M and p^M obtained by measuring different copies of the ensemble can be different. The magnitude of the distance measure d_1 signifies how well the mean (q_0, p_0) of the Gaussian state has been estimated. We define another distance measure d_2 for the accuracy estimation of the variance of the Gaussian state as

$$d_2 = \langle (V_q^A - V_q^M)^2 \rangle + \langle (V_p^A - V_p^M)^2 \rangle, \quad (53)$$

where V_q^A and V_p^A are the actual values of the variance of \hat{q} and \hat{p} quadratures, while V_q^M and V_p^M are the measured values of the variance of \hat{q} and \hat{p} quadratures. Here d_2 signifies how well the variance $(\Delta q)^2$ and $(\Delta p)^2$ has been estimated. In the case of perfect estimation, both distance measures d_1 and d_2 should approach zero.

A. Analytical expressions of distance measure d_1

Now we evaluate the distance measure d_1 for various measurement schemes, which are employed for the estimation of Gaussian states.

1. Homodyne measurement

To estimate the state using the homodyne measurement, we divide the ensemble in two halves. On the first half of the ensemble, the \hat{q} quadrature is measured, while on the other half of the ensemble, the \hat{p} quadrature is measured. Thus, we can write the distance measure d_1 for the homodyne measurement using Eqs. (19) and (21) as

$$d_1^{\text{Hom}} = \frac{(\Delta q)^2}{N/2} + \frac{(\Delta p)^2}{N/2}. \quad (54)$$

Here we have used the fact that the probability distribution involved in the homodyne measurement is Gaussian, and the sample variance for a Gaussian (normal) distribution $\mathcal{N}(\mu, \sigma)$ with mean μ and variance σ^2 for a sample of size N is given by σ^2/N .

2. Heterodyne measurement

The distance measure d_1 for the heterodyne measurement can be calculated using Eq. (25) and is given as

$$d_1^{\text{Het}} = \frac{(\Delta q)^2 + 1/2}{N} + \frac{(\Delta p)^2 + 1/2}{N}. \quad (55)$$

We can show analytically from Eqs. (54) and (55) that $d_1^{\text{Hom}} \geq d_1^{\text{Het}}$, where the equality sign holds only for a coherent state ensemble. Therefore, the homodyne measurement and the heterodyne measurement perform the same for a coherent state ensemble, whereas the heterodyne measurement outperforms

the homodyne measurement for a squeezed state ensemble as far as the mean estimation is concerned.

3. Sequential measurement scheme

For the sequential measurement scheme, we again divide the ensemble in two halves and perform the measurement according to the procedure described in Sec. II B 3. In this case the expression of the distance measure d_1 turns out to be

$$d_1^{\text{SM}} = \left\langle \left(q^A - \frac{q_1^M + q_2^M}{2} \right)^2 \right\rangle + \left\langle \left(p^A - \frac{p_1^M + p_2^M}{2} \right)^2 \right\rangle, \quad (56)$$

which can be rewritten as follows using Eqs. (36), (38), and (43):

$$d_1^{\text{SM}} = \frac{(\Delta q)^2 + (\Delta p)^2 + (\Delta Q_1)^2 + (\Delta P_1)^2}{N}. \quad (57)$$

It can be seen from the above equation that the optimal performance in the mean estimation for the sequential measurement scheme corresponds to $\Delta Q_1 = \Delta P_1 = 1/\sqrt{2}$. Further, at the optimal conditions, $d_1^{\text{SM}} = d_1^{\text{Het}}$.

4. Arthurs-Kelly measurement scheme

For the Arthurs-Kelly measurement scheme, we write the expression of distance measure d_1 using Eq. (51) as

$$d_1^{\text{AK}} = \frac{(\Delta q)^2 + (\Delta Q_1)^2 + \frac{(\Delta Q_2)^2}{4}}{N} + \frac{(\Delta p)^2 + \frac{(\Delta P_1)^2}{4} + (\Delta P_2)^2}{N}. \quad (58)$$

For the Arthurs-Kelly measurement scheme, the optimal performance in the mean estimation corresponds to

$$\Delta Q_1 = 1/2, \quad \Delta P_2 = 1/2, \quad (59)$$

and at the optimal conditions, $d_1^{\text{AK}} = d_1^{\text{Het}}$. This means that the optimal performance in the mean estimation of the sequential measurement requires only classical resources, i.e., the meter should be prepared in a coherent state, while the Arthurs-Kelly measurement scheme requires nonclassical resources, i.e., the meters should be prepared in a squeezed state.

Now we illustrate the dependence of the distance measure d_1 on the initial width of the meter ΔQ_1 , the squeezing parameter r , and the average number of photons $\langle n \rangle$ graphically. We have considered an ensemble of size $N = 20$ in the various figures in this article. We show the plot of the distance measure d_1 as a function of the initial width of the meter ΔQ_1 for a coherent state ensemble in Fig. 3(a). The results show that the homodyne measurement and the heterodyne measurement perform the same, and the optimal performance of the Arthurs-Kelly and sequential measurement schemes are equal to that of the homodyne measurement and the heterodyne measurement. Similarly, Fig. 3(b) shows the plot of distance measure d_1 as a function of the initial width of the meter ΔQ_1 for a squeezed coherent state ensemble with squeezing parameter $r = 1$. In this case, the heterodyne measurement outperforms the homodyne measurement. Further, an increase or a decrease in the size of the ensemble changes only the magnitude of the distance measure, while the performance

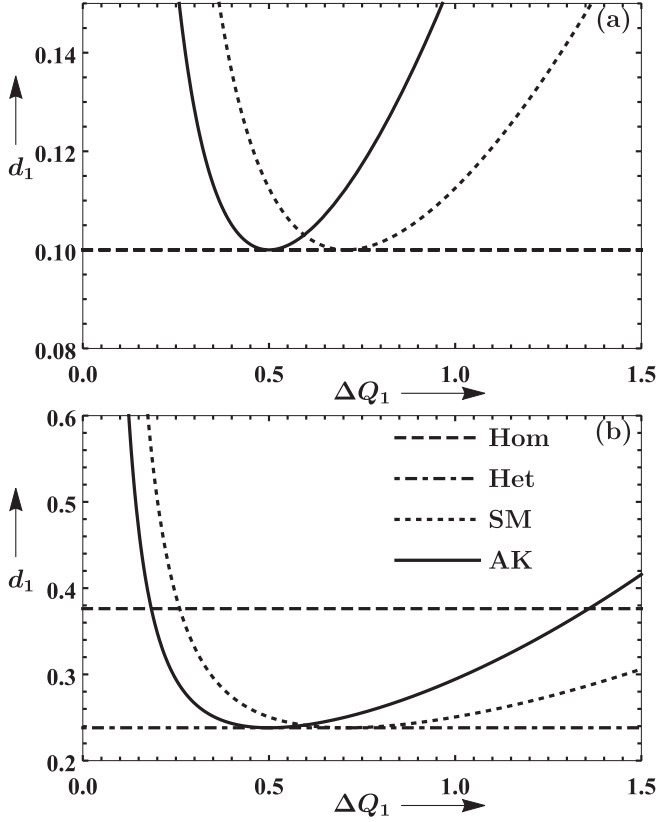


FIG. 3. Both panels show the distance measure d_1 as a function of the initial width of the meter ΔQ_1 for an ensemble of size $N = 20$. Additionally, we have taken $\Delta P_2 = 1/2$ in all the graphs for the Arthurs-Kelly measurement scheme, which is the condition for the optimal performance (59). (a) The ensemble consists of identically prepared coherent states. The homodyne measurement and the heterodyne measurement perform equally in this case. (b) The ensemble consists of identically prepared squeezed coherent states with squeezing parameter $r = 1$.

trend of the various measurement schemes remains the same. It should be noted that these conclusions about the relative performances of the various measurement schemes are based on the mean estimation efficacy. We plot the distance measure d_1 as a function of the squeezing parameter r in Fig. 4(a). The results show that both the homodyne measurement and the heterodyne measurement estimate the mean of the Gaussian state with the same distance measure for a coherent state ensemble ($r = 0$), while for a squeezed coherent state ensemble ($r > 0$), the heterodyne measurement outperforms the homodyne measurement. The plot of the distance measure d_1 as a function of the average number of photons $\langle n \rangle$ is shown in Fig. 4(b). The results show that the distance measure of the mean estimation increases, i.e., the estimation efficiency decreases, for a thermal state ($\langle n \rangle > 0$) ensemble as compared to a pure state ($\langle n \rangle = 0$) ensemble.

B. Analytical expressions of distance measure d_2

We now proceed to derive expressions of distance measure d_2 (53) for all the measurement schemes.

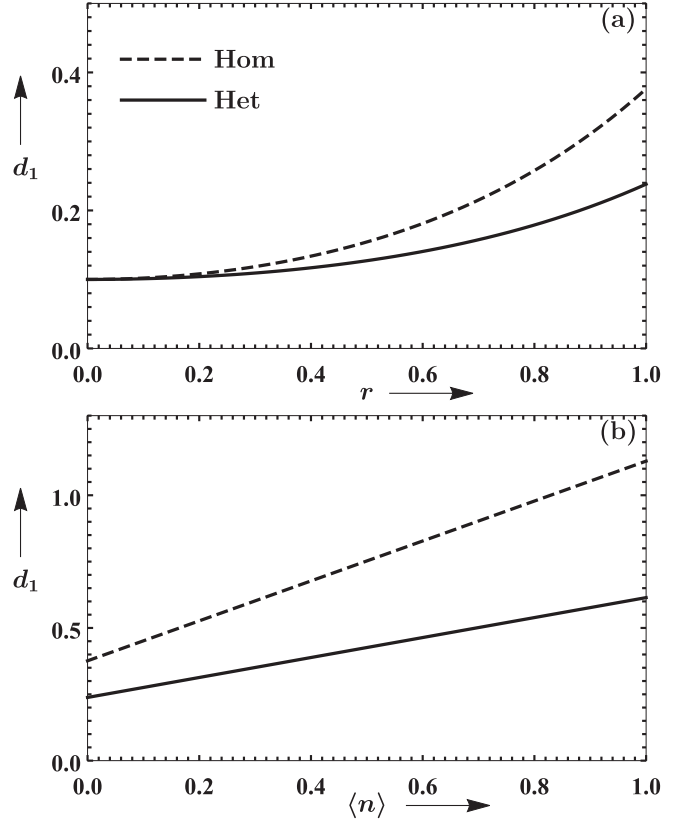


FIG. 4. (a) The distance measure d_1 as a function of the squeezing parameter r . The average number of photons is $\langle n \rangle = 0$. (b) The distance measure d_1 as a function of the average number of photons $\langle n \rangle$. The squeezing parameter has been taken as $r = 1$. An ensemble of size $N = 20$ has been considered for both panels.

1. Homodyne measurement

For the homodyne measurement, the expression of the distance measure d_2 evaluates to

$$d_2^{\text{Hom}} = \frac{2(\Delta q)^4}{N/2} + \frac{2(\Delta p)^4}{N/2}. \quad (60)$$

Here we have used the fact that the variance of the sample variance for a Gaussian (normal) distribution $\mathcal{N}(\mu, \sigma)$ with mean μ and variance σ^2 for a sample of size N is given by $2\sigma^4/N$.

2. Heterodyne measurement

The expression of the distance measure d_2 for the heterodyne measurement evaluates to

$$d_2^{\text{Het}} = \frac{2[(\Delta q)^2 + 1/2]^2}{N} + \frac{2[(\Delta p)^2 + 1/2]^2}{N}. \quad (61)$$

The expansion of d_2^{Het} provides additional terms besides $(\Delta q)^4$ and $(\Delta p)^4$, which renders d_2^{Het} larger than d_2^{Hom} . The distance measures d_2 for these two measurements cross over each other at a certain threshold squeezing, below which homodyne measurement performs better than heterodyne measurement. The explicit expression for the threshold squeezing is provided in Eq. (64), and the crossover is illustrated in Fig. 6 below.

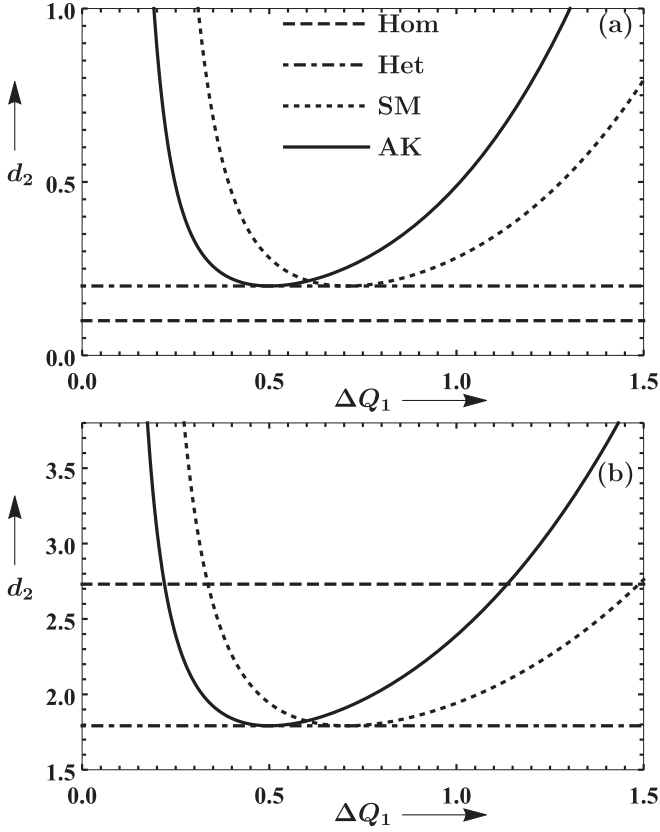


FIG. 5. Both panels show the distance measure d_2 as a function of the initial width of the meter ΔQ_1 for an ensemble of size $N = 20$. (a) The ensemble consists of identically prepared coherent states. (b) The ensemble consists of identically prepared squeezed coherent states with squeezing parameter $r = 1$.

This behavior is in stark contrast with the behavior of distance measure d_1 for homodyne and heterodyne measurements, which can be explained as follows. As we can see from Eq. (25), heterodyne measurement results in the addition of vacuum noise to the variances of \hat{q} and \hat{p} quadratures. We note that d_1 and d_2 are proportional to the variance and variance squared of the corresponding measurement probability distribution. This dependence on variance and variance squared coupled with the fact that the heterodyne measurement results in the addition of noise to the variance leads to the contrasting behavior.

3. Sequential measurement scheme

For the sequential measurement scheme, the expression of the distance measure d_2 can be written in an analogous way as Eq. (56). The final expression of the distance measure in this case evaluates to

$$d_2^{\text{SM}} = \frac{2}{N} \{ (\Delta p)^4 + (\Delta q)^2 [(\Delta Q_1)^2 + (\Delta q)^2]^2 + (\Delta P_1)^2 [(\Delta q)^2 + (\Delta p)^2 + (\Delta P_1)^2]^2 + (\Delta Q_1)^2 [(\Delta Q_1)^2 + (\Delta p)^2]^2 \}. \quad (62)$$

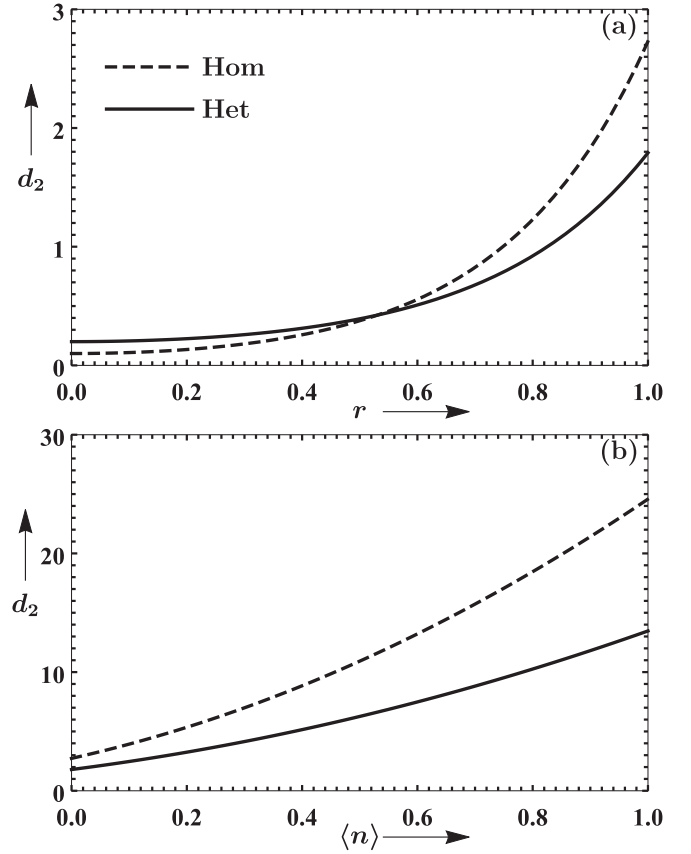


FIG. 6. (a) The distance measure d_2 as a function of the squeezing parameter r . The average number of photons has been set as $\langle n \rangle = 0$. (b) The distance measure d_2 as a function of the average number of photons $\langle n \rangle$. The squeezing parameter has been taken as $r = 1$. An ensemble of size $N = 20$ has been considered for both panels.

4. Arthurs-Kelly measurement scheme

Similarly, the distance measure d_2 for the Arthurs-Kelly measurement scheme can be calculated and turns out to be

$$d_2^{\text{AK}} = \frac{2[(\Delta q)^2 + (\Delta Q_1)^2 + \frac{(\Delta Q_2)^2}{4}]^2}{N} + \frac{2[(\Delta p)^2 + \frac{(\Delta P_1)^2}{4} + (\Delta P_2)^2]^2}{N}. \quad (63)$$

We note here that the distance measures d_1 and d_2 for different measurement schemes are independent of the actual values of the mean q_0 and p_0 of the Gaussian states and depend only on the actual variances $(\Delta q)^2$ and $(\Delta p)^2$ of the quadratures. Now we turn to study the dependence of distance measure d_2 on the initial width of the meter ΔQ_1 , the squeezing parameter r , and the average number of photons $\langle n \rangle$ as we did for d_1 .

We show the plot of the distance measure d_2 as a function of the initial width of the meter ΔQ_1 for a coherent state ensemble in Fig. 5(a). The results show that the homodyne measurement outperforms the heterodyne measurement in estimating the variance for a coherent state ensemble. We also notice that the optimal performance of the Arthurs-Kelly and sequential measurement schemes equals the heterodyne measurement. We note that the optimal performance of the

Arthurs-Kelly measurement scheme occurs at $\Delta Q_1 = \Delta P_2 = 1/2$, while the optimal performance of the sequential measurement scheme occurs at $\Delta Q_1 = 1/\sqrt{2}$.

Similarly, Fig. 5(b) shows the plot of the distance measure d_2 as a function of the initial width of the meter ΔQ_1 for a squeezed coherent state ensemble with squeezing parameter $r = 1$. The results show that the heterodyne measurement outperforms the homodyne measurement in estimating the variance of a squeezed state ensemble with squeezing parameter $r = 1$. Here, too, the optimal performance of the Arthurs-Kelly measurement scheme and the sequential measurement equal the heterodyne measurement. We plot the distance measure d_2 as a function of the squeezing parameter r in Fig. 6(a) for $\langle n \rangle = 0$. The results show that the homodyne measurement outperforms the heterodyne measurement up to a certain value of the squeezing parameter $r_c = 0.53$. This result is in contrast with the distance measure d_1 result, where the heterodyne measurement outperforms the homodyne measurement for all nonzero squeezing parameters. The critical value of the squeezing parameter r_c at a given $\langle n \rangle$, where the relative performance of the homodyne measurement is equal to the heterodyne measurement can be written as

$$e^{2r_c} = \frac{1 + \sqrt{3 + 2n_1^2} + \sqrt{2(2 - n_1^2 + \sqrt{3 + 2n_1^2})}}{2n_1}, \quad (64)$$

where $n_1 = 2\langle n \rangle + 1$. Further, the plot of the distance measure d_2 as a function of the average number of photons $\langle n \rangle$ is shown in Fig. 6(b). The results reveal that the variance estimation for a thermal state ensemble is less precise as compared to a pure state ensemble.

C. Average estimation efficiency

It is important to know how different schemes perform on the average. To achieve this we compare the relative performances of the measurement schemes under consideration on a large number of randomly generated squeezed coherent thermal states with squeezing parameter r varying uniformly between -1 and $+1$. Such an ensemble can be produced by a parametric down converter operating at a fixed temperature, which generates states with squeezing parameter r uniformly distributed between -1 and $+1$. We note that the squeezing parameter range -1 to $+1$ can be easily achieved in experiments. For evaluating the average distance measures \bar{d}_1 and \bar{d}_2 , we consider the state of the system to be parameterized by the squeezing parameter r and the average number of photons $\langle n \rangle$ as given in Eq. (16).

1. Calculation of mean distance measure \bar{d}_1

The mean distance measure \bar{d}_1 for the homodyne measurement is calculated as

$$\bar{d}_1^{\text{Hom}} = \frac{1}{2} \int_{-1}^{+1} d_1^{\text{Hom}}(r, \langle n \rangle) dr, = \frac{n_1 \sinh(2)}{N}, \quad (65)$$

where $n_1 = 2\langle n \rangle + 1$. Similarly, the final expressions of the average distance measure \bar{d}_1 for the other measurement

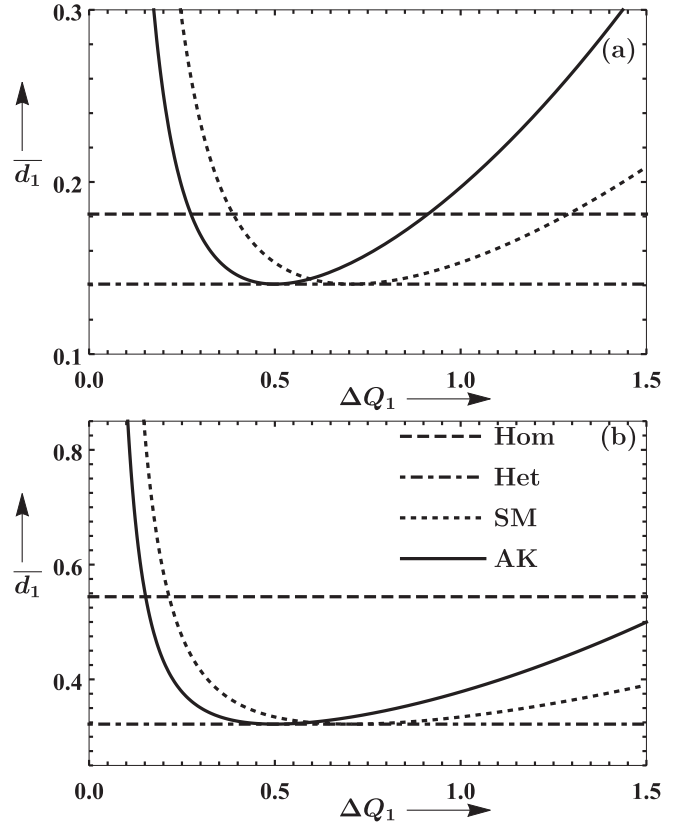


FIG. 7. Both panels show the mean distance measure \bar{d}_1 as a function of the initial width of the meter ΔQ_1 for an ensemble of size $N = 20$. (a) The averaging is done over the identically prepared pure squeezed coherent state ($\langle n \rangle = 0$), whose squeezing parameter r is uniformly distributed between -1 and $+1$. (b) The averaging is done over an identically prepared squeezed coherent thermal state with $\langle n \rangle = 1$, whose squeezing parameter r is uniformly distributed between -1 and $+1$.

schemes are

$$\begin{aligned} \bar{d}_1^{\text{Het}} &= \frac{2 + n_1 \sinh(2)}{2N}, \\ \bar{d}_1^{\text{SM}} &= \frac{2[(\Delta Q_1)^2 + (\Delta P_1)^2] + n_1 \sinh(2)}{2N}, \\ \bar{d}_1^{\text{AK}} &= \frac{1}{4N} \{(\Delta Q_2)^2 + (\Delta P_1)^2 + 4[(\Delta Q_1)^2 + (\Delta P_2)^2] \\ &\quad + 2n_1 \sinh(2)\}. \end{aligned} \quad (66)$$

The results for the mean distance measure \bar{d}_1 for various measurement schemes are shown in Fig. 7. We see from Fig. 7(a) that the heterodyne measurement outperforms the homodyne measurement, and the optimal performance of the Arthurs-Kelly and sequential measurement schemes equals the heterodyne measurement. Figure 7(b) shows that the performance trend for the thermal state ensembles is similar to the pure state ensembles except that the distance measure of the mean \bar{d}_1 is reduced for the thermal state ensemble as compared to the pure state ensemble.

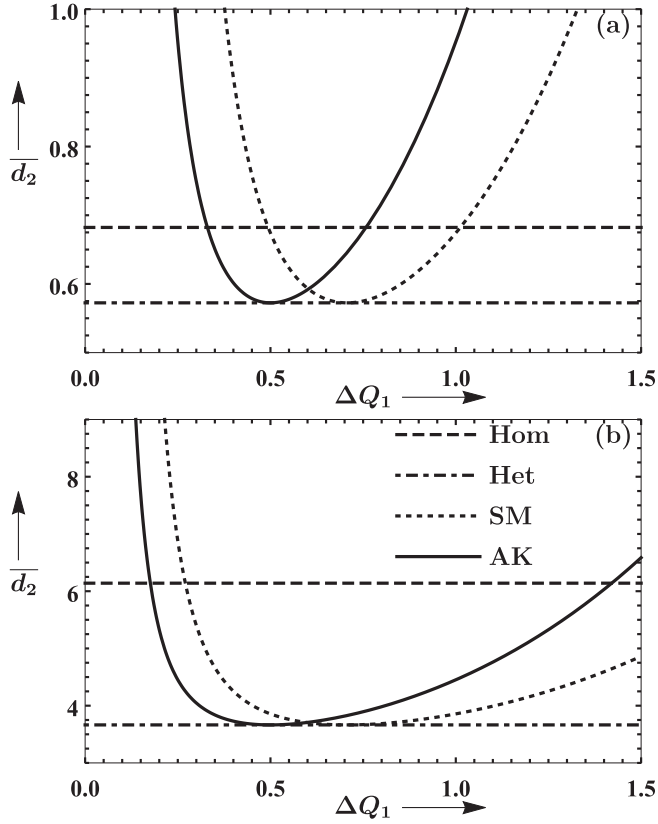


FIG. 8. Both panels show the mean distance measure \bar{d}_2 as a function of the initial width of the meter ΔQ_1 for an ensemble of size $N = 20$. (a) The averaging is done over an identically prepared pure squeezed coherent state ($\langle n \rangle = 0$), whose squeezing parameter r is uniformly distributed between -1 and $+1$. (b) The averaging is done over an identically prepared squeezed coherent thermal state with $\langle n \rangle = 1$, whose squeezing parameter r is uniformly distributed between -1 and $+1$.

2. Calculation of mean distance measure \bar{d}_2

We now calculate the expressions of the mean distance measure \bar{d}_2 averaged over different squeezed coherent thermal state ensembles with squeezing parameter r uniformly distributed between -1 and $+1$ for different measurement schemes. The mean distance measure \bar{d}_2 for the homodyne measurement and the heterodyne measurement evaluate to

$$\begin{aligned} \bar{d}_2^{\text{Hom}} &= \frac{n_1^2 \sinh(4)}{2N}, \\ \bar{d}_2^{\text{Het}} &= \frac{4 + 4n_1 \sinh(2) + n_1^2 \sinh(4)}{4N}. \end{aligned} \quad (67)$$

Similarly, the expressions of the mean distance measure \bar{d}_2 for the sequential and the Arthurs-Kelly measurement schemes evaluate to

$$\begin{aligned} \bar{d}_2^{\text{SM}} &= \frac{1}{4N} \{4[(\Delta Q_1)^2 + (\Delta P_1)^2][2 + n_1 \sinh(2)] \\ &\quad + n_1^2 \sinh(4)\}, \end{aligned}$$

TABLE I. Homodyne measurement versus heterodyne measurement. d_1 and d_2 represent the accuracy of the mean and the variance estimation, respectively.

Ensemble	Distance measure	Relative performance
Coherent state ($r = 0$)	$d_1^{\text{Hom}} = d_1^{\text{Het}}$	Hom = Het
Squeezed state ($r > 0$)	$d_1^{\text{Hom}} > d_1^{\text{Het}}$	Hom < Het
$r < r_c$ [Eq. (64)]	$d_2^{\text{Hom}} < d_2^{\text{Het}}$	Hom > Het
$r > r_c$	$d_2^{\text{Hom}} > d_2^{\text{Het}}$	Hom < Het
$-1 \leq r \leq +1$	$\bar{d}_1^{\text{Hom}} > \bar{d}_1^{\text{Het}}$	Hom < Het
$-1 \leq r \leq +1$	$\bar{d}_2^{\text{Hom}} > \bar{d}_2^{\text{Het}}$	Hom < Het

$$\begin{aligned} \bar{d}_2^{\text{AK}} &= \frac{1}{8N} \{ [4(\Delta Q_1)^2 + (\Delta Q_2)^2 + 2n_1 \sinh(2)] \\ &\quad \times [4(\Delta Q_1)^2 + (\Delta Q_2)^2] + [(\Delta P_1)^2 + 4(\Delta P_2)^2] \\ &\quad \times [(\Delta P_1)^2 + 4(\Delta P_2)^2 + 2n_1 \sinh(2)] + 2n_1^2 \sinh(4) \}. \end{aligned} \quad (68)$$

The results for the mean distance measure \bar{d}_2 for various measurement schemes are shown in Fig. 8. As can be seen from Fig. 8(a), the heterodyne measurement outperforms the homodyne measurement, and the optimal performance of the Arthurs-Kelly and sequential measurement schemes equals the heterodyne measurement. For the thermal state ensembles, the performance trend remains the same; however, the distance measure of the variance \bar{d}_2 is reduced for the thermal state ensembles as compared to the pure state ensembles as can be seen from Fig. 8(b).

We summarize the relative performances of the homodyne measurement and the heterodyne measurement in Table I. We further note that the optimal performance of the sequential and the Arthurs-Kelly measurement schemes is equal to the heterodyne measurement for both the mean and the variance estimation.

D. Environmental interactions and imperfect detectors

In this subsection, we consider that the ensemble interacts with a thermal bath. The associated interaction Hamiltonian is

$$\hat{H}_{SB} = g \sum_{k=1}^{\infty} (\hat{a} \hat{b}_k^\dagger + \hat{a}^\dagger \hat{b}_k), \quad (69)$$

where g is the coupling constant and \hat{b}_k represents the annihilation operator of the k th mode of the bath interacting with the system. The master equation for the evolution of system density operator ρ under Markovian assumption can be written as

$$\begin{aligned} \frac{\partial}{\partial t} \rho &= \frac{\gamma}{2} (N_B + 1) (2\hat{a} \rho \hat{a}^\dagger - \hat{a}^\dagger \hat{a} \rho - \rho \hat{a}^\dagger \hat{a}) \\ &\quad + \frac{\gamma}{2} N_B (2\hat{a}^\dagger \rho \hat{a} - \hat{a} \hat{a}^\dagger \rho - \rho \hat{a} \hat{a}^\dagger), \end{aligned} \quad (70)$$

where γ is the decay constant and N_B is the mean photon number of the thermal bath. The evolution of the displacement vector $\hat{\xi}$ and covariance matrix V after an interaction for time t with the thermal bath can be evaluated using the master

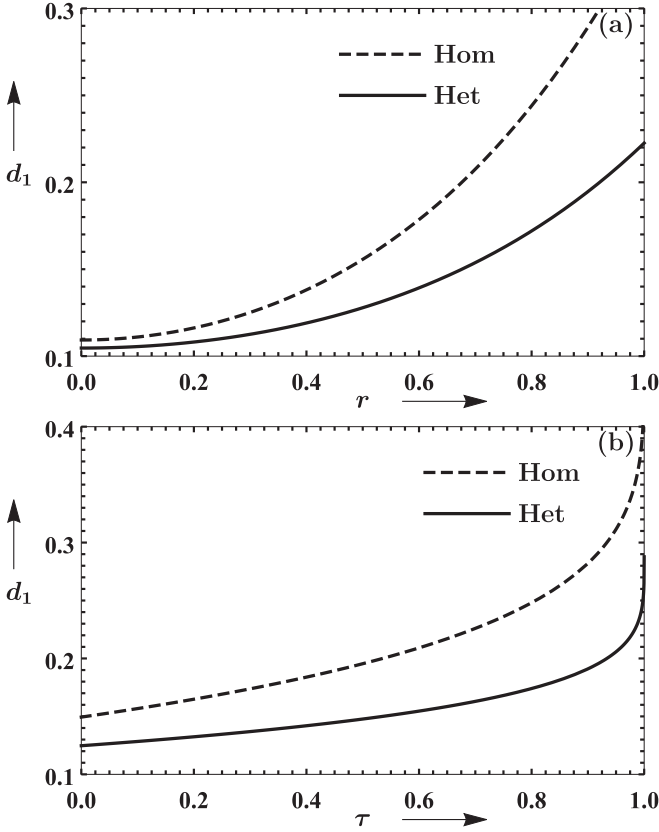


FIG. 9. (a) The distance measure d_1 as a function of the squeezing parameter r . We have set $\tau = 0.1$. (b) The distance measure d_1 as a function of the dimensionless time parameter τ . We have set $r = 0.5$. Other parameters have been set as $\langle n \rangle = 0$, $N = 20$, $N_B = 4$, $q_0 = 1$, $p_0 = 1$, and $\eta = 0.9$ for both panels.

Eq. (70), which turns out to be [48]

$$\bar{\xi}'(t) = X(t)\bar{\xi}, \quad V'(t) = X(t)V(0)X(t)^T + \frac{1}{2}Y(t), \quad (71)$$

where $X(t)$ and $Y(t)$ are given by

$$X(t) = (1 - \tau)^{1/4} \mathbb{1}_2, \quad Y(t) = \left(1 + \frac{N_B}{2}\right)(1 - \sqrt{1 - \tau}) \mathbb{1}_2, \quad (72)$$

with $\tau = 1 - e^{-2\gamma t}$ being a dimensionless time parameter. Further, while t runs from 0 to ∞ , τ runs from 0 to 1.

We also consider imperfect detectors with nonunit quantum efficiency η . Such detectors (without dark counts) can be modeled by a beam splitter of transmissivity η followed by an ideal detector of unit quantum efficiency. The displacement vector $\bar{\xi}'(t)$ and the covariance matrix $V'(t)$ further evolves to

$$\bar{\xi}''(t) = \sqrt{\eta}\bar{\xi}'(t), \quad V''(t) = \eta V'(t) + \frac{1}{2}(1 - \eta)\mathbb{1}_2. \quad (73)$$

Since, at optimal performance, the Arthurs-Kelly and sequential measurement schemes yield the same results as that of the heterodyne measurement, therefore we consider only homodyne and heterodyne measurements in this subsection.

We first analyze the distance measure d_1 with respect to the squeezing of the state and time τ . It should be noted that

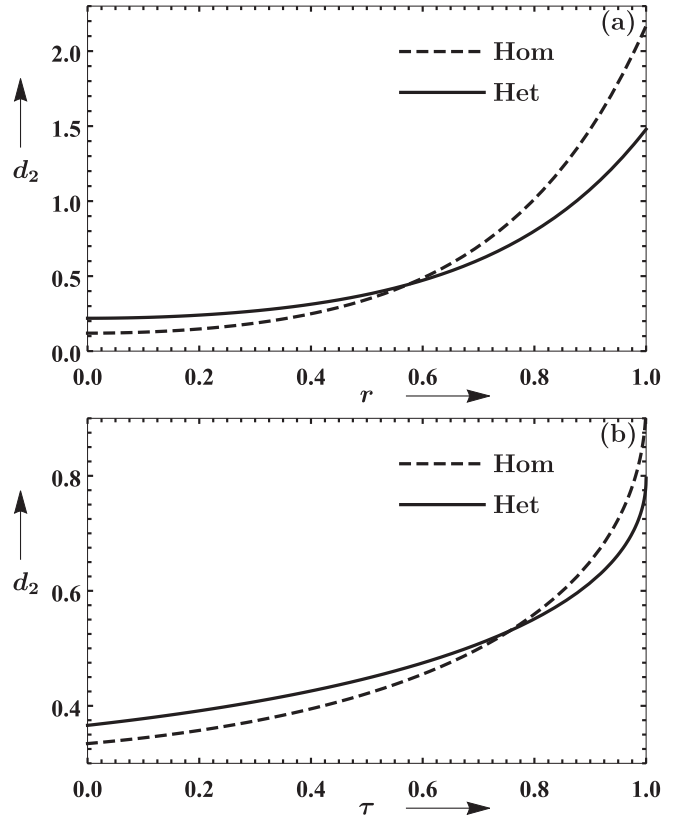


FIG. 10. (a) The distance measure d_2 as a function of the squeezing parameter r . We have set $\tau = 0.1$. (b) The distance measure d_2 as a function of the dimensionless time parameter τ . We have set $r = 0.5$. Other parameters have been set as $\langle n \rangle = 0$, $N = 20$, $N_B = 4$, and $\eta = 0.9$ for both panels.

d_1 also depends on the initial displacement $\bar{\xi} = (q_0, p_0)^T$ of the state (14), which is in contrast with the results in the earlier sections. As shown in Fig. 9(a), heterodyne measurement outperforms homodyne measurement for all squeezing, including $r = 0$, which is contrary to the estimation of pure Gaussian states, where homodyne and heterodyne measurements perform equally at $r = 0$. The plot for the distance measure d_1 as a function of τ is shown in Fig. 9(b). The results reveal that the performance of both homodyne and heterodyne measurements degrades as τ is increased. On comparing the derivative of the distance measure d_1 with τ for homodyne and heterodyne measurements, we find that the heterodyne measurement is more robust for all interaction times.

We now study the distance measure d_2 with respect to the squeezing r and time τ . As we can see from Fig. 10(a), homodyne measurement outperforms heterodyne measurement up to a certain squeezing threshold, which is similar to the estimation of pure Gaussian states. Now we plot the distance measure d_2 with respect to τ in Fig. 10(b). It can be seen that the performance of both measurements decreases as τ is increased. Further, on comparing the derivative of the distance measure d_2 with τ for homodyne and heterodyne measurements, we find that the homodyne measurement is more robust up to a certain τ beyond which the heterodyne measurement is more robust.

IV. MODIFIED HAMILTONIAN IN THE ARTHURS-KELLY MEASUREMENT SCHEME

The Arthurs-Kelly measurement scheme has two measuring probes. What if these probes can influence each other and are correlated [37]? To this end, we consider a modified form of the interaction Hamiltonian [37,38] in the Arthurs-Kelly measurement scheme

$$H = \delta(t - t_1) \left(\hat{q} \hat{P}_1 - \hat{p} \hat{Q}_2 + \frac{\kappa}{2} \hat{P}_1 \hat{Q}_2 \right), \quad (74)$$

where κ determine the coupling strength between the two probes. This Hamiltonian entangles the system with both meters as well as the two meters between themselves. The corresponding symplectic transformation acting on the

$$V_{M_1 M_2}^{\text{RED}} = \begin{pmatrix} V_{M_1}(Q_1) & 0 & \frac{(\kappa-1)}{2}(\Delta Q_2)^2 & 0 \\ 0 & (\Delta P_1)^2 & 0 & -\frac{(\kappa+1)}{2}(\Delta P_1)^2 \\ \frac{(\kappa-1)}{2}(\Delta Q_2)^2 & 0 & (\Delta Q_2)^2 & 0 \\ 0 & -\frac{(\kappa+1)}{2}(\Delta P_1)^2 & 0 & V_{M_2}(P_2) \end{pmatrix}, \quad (76)$$

where

$$V_{M_1}(Q_1) = (\Delta q)^2 + (\Delta Q_1)^2 + \frac{(\kappa-1)^2}{4}(\Delta Q_2)^2, \\ V_{M_2}(P_2) = (\Delta p)^2 + \frac{(\kappa+1)^2}{4}(\Delta P_1)^2 + (\Delta P_2)^2. \quad (77)$$

We find, using Simon's entanglement criteria [49], that the reduced state of the two meters is entangled for $|\kappa| \geq 1$. The variance of the probability distribution for the measurement of the \hat{q} quadrature on meter 1 and the \hat{p} quadrature on meter 2 can be written as the variance corresponding to \hat{Q}_1 and \hat{P}_2 in the covariance matrix for the reduced state of the meters (76):

$$V^{\text{COR}}(\hat{q}) = (\Delta q)^2 + (\Delta Q_1)^2 + \frac{(\kappa-1)^2}{4}(\Delta Q_2)^2, \\ V^{\text{COR}}(\hat{p}) = (\Delta p)^2 + \frac{(\kappa+1)^2}{4}(\Delta P_1)^2 + (\Delta P_2)^2. \quad (78)$$

Thus, the distance measure d_1 for the modified Arthurs-Kelly measurement scheme reads

$$d_1^{\text{COR}} = \frac{V^{\text{COR}}(\hat{q})}{N} + \frac{V^{\text{COR}}(\hat{p})}{N}. \quad (79)$$

We optimize the distance measure d_1^{COR} with respect to the parameters ΔQ_1 and ΔP_2 . The optimal value of the distance measure d_1^{COR} evaluates to

$$d_{1\text{OPT}}^{\text{COR}} = \begin{cases} \frac{1+(\Delta q)^2+(\Delta p)^2}{N} & |\kappa| \leq 1, \\ \frac{|\kappa|+(\Delta q)^2+(\Delta p)^2}{N} & |\kappa| > 1. \end{cases} \quad (80)$$

We note that the optimal distance measure $d_{1\text{OPT}}^{\text{COR}}$ for $|\kappa| \leq 1$ equals the distance measure for the heterodyne measurement

quadrature operators is

$$S = \begin{pmatrix} q & p & Q_1 & P_1 & Q_2 & P_2 \\ \hline 1 & 0 & 0 & 0 & -1 & 0 \\ 0 & 1 & 0 & -1 & 0 & 0 \\ \hline 1 & 0 & 1 & 0 & \frac{\kappa-1}{2} & 0 \\ 0 & 0 & 0 & 1 & 0 & 0 \\ \hline 0 & 0 & 0 & 0 & 1 & 0 \\ 0 & 1 & 0 & \frac{-\kappa-1}{2} & 0 & 1 \end{pmatrix} \begin{matrix} q \\ p \\ Q_1 \\ P_1 \\ Q_2 \\ P_2 \end{matrix}, \quad (75)$$

The covariance matrix and the displacement vector corresponding to system-meters state after time t_1 can be evaluated using Eq. (13). The covariance matrix of the reduced state of the two meters is given by

d_1^{Het} (55).

The plot of the distance measure d_1 as a function of the coupling strength κ for a coherent state ensemble is shown in Fig. 11(a). The results show that the estimation of the coherent state ensemble using the modified Arthurs-Kelly measurement scheme is best in the range $|\kappa| \leq 1$, which corresponds to uncorrelated probes. The corresponding value of ΔQ_1 and ΔP_2 , which optimizes the distance measure d_1^{COR} , turns out to be

$$\Delta Q_1 = \begin{cases} \frac{\sqrt{1+\kappa}}{2} & \kappa > 1, \\ \frac{\sqrt{1+\kappa}}{2} & |\kappa| < 1, \\ \frac{\sqrt{-1-\kappa}}{2} & \kappa < -1, \end{cases} \quad \Delta P_2 = \begin{cases} \frac{\sqrt{-1+\kappa}}{2} & \kappa > 1, \\ \frac{\sqrt{1-\kappa}}{2} & |\kappa| < 1, \\ \frac{\sqrt{1-\kappa}}{2} & \kappa < -1. \end{cases} \quad (81)$$

We have also plotted ΔQ_1 and ΔP_2 as a function of the coupling strength κ corresponding to the optimal performance of the modified Arthurs-Kelly measurement scheme in Fig. 11(b). For the coupling strength $\kappa = 0$, the modified Arthurs-Kelly measurement scheme reduces to the original Arthurs-Kelly measurement scheme. This can also be verified from Fig. 11(b), where at $\kappa = 0$, $\Delta Q_1 = \Delta P_1 = 1/2$, which is the same as Eq. (59).

Furthermore, the analysis for the distance measure d_2 also shows that the estimation of the coherent state ensemble using the modified Arthurs-Kelly measurement scheme is best in the range $|\kappa| \leq 1$.

V. DISCUSSION AND CONCLUSION

In this paper, we have explored the estimation of the mean and the variance of an ensemble of a fixed number of identically prepared Gaussian states by employing four different measurement schemes with a view to compare their efficiencies. Since we were dealing with Gaussian states and

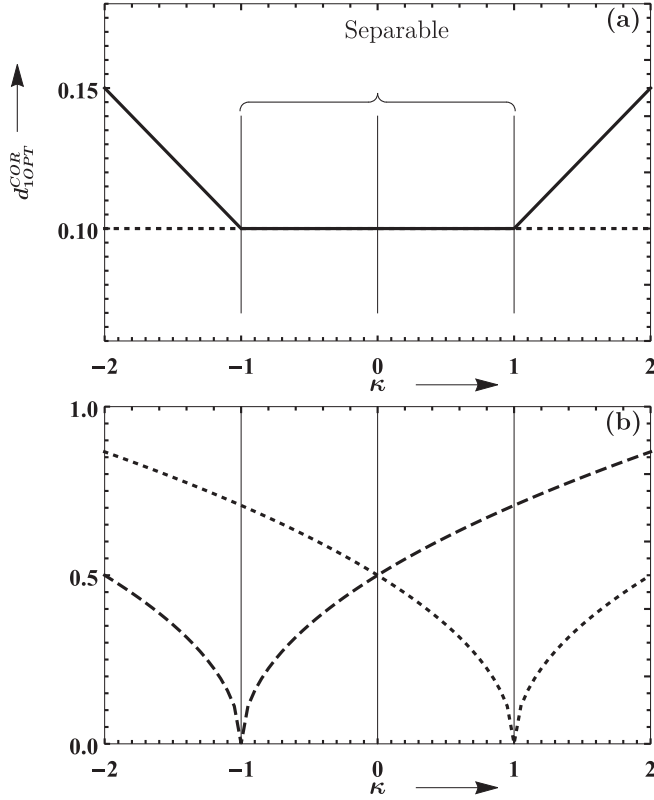


FIG. 11. (a) Optimal distance measure $d_{1,OPT}^{COR}$ for the modified Arthurs-Kelly measurement scheme, represented by the solid curve, as a function of the coupling strength κ . The dashed curve represents the distance measure for the heterodyne measurement d_1^{Het} . (b) ΔQ_1 (dashed) and ΔP_2 (dotted) for the optimal performance of the modified Arthurs-Kelly measurement scheme as a function of the coupling strength κ . We have considered an ensemble of coherent states for both panels.

quadratic Hamiltonians, the covariance matrix, phase space formulation, and symplectic group techniques provided an elegant and intuitive way to handle the analysis. Detailed analysis of the distance measures revealed that the optimal performance of the Arthurs-Kelly measurement scheme requires nonclassical resources in the sense that the meters should be initially prepared in a squeezed state; however, the optimal performance of the sequential measurement scheme requires only classical resources, i.e., the meter should be initially prepared in a coherent state. Further, we showed that the optimal performance of the Arthurs-Kelly and sequential measurement schemes equal heterodyne measurement for both the mean and the variance estimation.

For mean estimation, the analysis revealed that the performance of the homodyne measurement and the heterodyne measurement is the same for a coherent state ensemble, whereas, for a squeezed state ensemble, the heterodyne measurement performs better than the homodyne measurement. For variance estimation, the homodyne measurement outperforms the heterodyne measurement for a squeezed coherent thermal state ensemble up to a certain squeezing parameter range. The results show that the heterodyne measurement always perform better than the homodyne measurement for both the mean and the variance estimation on the average.

We considered the possibility of correlated probes for the Arthurs-Kelly measurement scheme and showed that optimal performance of the scheme can be obtained only when the meters are uncorrelated.

We also investigated the effects of environmental interactions and imperfect detectors. We observed that the precision of the homodyne and heterodyne measurements decreases as the interaction time increases. We also observed that the heterodyne measurement is more robust for the distance measure d_1 at all interaction times, while for distance measure d_2 , the heterodyne measurement is more robust beyond a certain interaction time.

Purification of noisy coherent state ensemble [50] have been carried out by performing arithmetic averaging of variance [51]. In this scheme, N identical noisy coherent states are combined using $N - 1$ beam splitters, and one of the output signals corresponds to the purified coherent state [51]. It would be interesting to compare the efficacy of various measurement schemes in the mean and variance estimation of the purified state with the original ensemble. One can also extend the analysis for Gaussian states squeezed in arbitrary directions and non-Gaussian states, where we are required to estimate higher order moments.

ACKNOWLEDGMENTS

C.K. thanks Shikhar Arora for his crucial remarks on the final version of the manuscript. A. and C.K. acknowledge the financial support from DST/ICPS/QuST/Theme-1/2019/General Project No. Q-68.

APPENDIX A: CALCULATION OF THE SYMPLECTIC TRANSFORMATION MATRIX FOR A GIVEN HAMILTONIAN

We provide two different methods to evaluate the symplectic transformation matrix for a given Hamiltonian.

1. Method I: Hilbert space and Baker-Campbell-Hausdorff formula

Consider the Hamiltonian $\hat{H}(t) = \delta(t - t_1)\hat{q}\hat{P}_1$ [Eq. (28)]. The corresponding infinite dimensional unitary operator for $t > t_1$ is given by

$$\mathcal{U}(\hat{H}(t)) = e^{-i \int \hat{H}(t) dt} = e^{-i\hat{q}\hat{P}_1}. \quad (\text{A1})$$

In the Heisenberg picture, the evolution of any operator \hat{A} can be written as

$$\hat{A} \xrightarrow{\mathcal{U}(\hat{H}(t))} \mathcal{U}(\hat{H}(t))^\dagger \hat{A} \mathcal{U}(\hat{H}(t)). \quad (\text{A2})$$

Thus, the transformation of various quadrature operators using the Baker-Campbell-Hausdorff (BCH) formula can be evaluated as following:

$$\begin{aligned} e^{i\hat{q}\hat{P}_1} \hat{q} e^{-i\hat{q}\hat{P}_1} &= \hat{q}, \\ e^{i\hat{q}\hat{P}_1} \hat{p} e^{-i\hat{q}\hat{P}_1} &= \hat{p} - \hat{P}_1, \\ e^{i\hat{q}\hat{P}_1} \hat{Q}_1 e^{-i\hat{q}\hat{P}_1} &= \hat{q} + \hat{Q}_1, \\ e^{i\hat{q}\hat{P}_1} \hat{P}_1 e^{-i\hat{q}\hat{P}_1} &= \hat{P}_1. \end{aligned} \quad (\text{A3})$$

Thus, the quadrature operators transform as

$$\begin{pmatrix} \hat{q} \\ \hat{p} \\ \hat{Q} \\ \hat{P}_1 \end{pmatrix} \xrightarrow{u(\hat{H}(t))} \underbrace{\begin{pmatrix} 1 & 0 & 0 & 0 \\ 0 & 1 & 0 & -1 \\ 1 & 0 & 1 & 0 \\ 0 & 0 & 0 & 1 \end{pmatrix}}_S \begin{pmatrix} \hat{q} \\ \hat{p} \\ \hat{Q} \\ \hat{P}_1 \end{pmatrix}, \quad (\text{A4})$$

where S is the symplectic transformation corresponding to the Hamiltonian $\hat{H}(t) = \delta(t - t_1)\hat{q}\hat{P}_1$. However, this method gets a little complicated for the modified Arthurs-Kelly measurement scheme, where the Hamiltonian is $H = \delta(t - t_1)(\hat{q}\hat{P}_1 - \hat{p}\hat{Q}_2 + \frac{\kappa}{2}\hat{P}_1\hat{Q}_2)$. Alternatively, we can take another approach where such complicated calculations can be performed easily.

2. Method II: Exponentiation of the generators of $\text{Sp}(2n, \mathcal{R})$

Let J be the generator of the symplectic group $\text{Sp}(2n, \mathcal{R})$, i.e., J is an element of the Lie algebra of $\text{Sp}(2n, \mathcal{R})$ group. The corresponding symplectic group element S can be obtained by exponentiating J as follows:

$$S = \exp(J). \quad (\text{A5})$$

We can associate a quadratic function of quadrature operators with every J , which is Hermitian, as follows:

$$H(J) = \frac{1}{2}\hat{\xi}^T(\Omega J)\hat{\xi}, \quad (\text{A6})$$

where $\hat{\xi}$ is the column of quadrature operators and Ω is the symplectic form. Since the generators of the symplectic group and quadratic functions of the quadrature operators are in one-to-one correspondence at Lie algebra level, we can exponentiate $H(J)$ to obtain infinite-dimensional unitary representation of $S = \exp(J)$. Thus, in our case, we can first determine the generator J from the given Hamiltonian and evaluate the corresponding symplectic transformation by exponentiation. We illustrate this procedure for the Hamiltonian $\hat{H}(t) = \delta(t - t_1)\hat{q}\hat{P}_1$, whose corresponding infinite dimen-

sional unitary representation is $e^{-i\hat{q}\hat{P}_1}$. We can write

$$-i\hat{q}\hat{P}_1 = \frac{1}{2}\hat{\xi}^T(\Omega J)\hat{\xi}, \quad (\text{A7})$$

where $\hat{\xi} = (\hat{q}, \hat{p}, \hat{Q}_1, \hat{P}_1)^T$ and

$$\Omega J = -\begin{pmatrix} 0 & 0 & 0 & 1 \\ 0 & 0 & 0 & 0 \\ 0 & 0 & 0 & 0 \\ 1 & 0 & 0 & 0 \end{pmatrix}. \quad (\text{A8})$$

Consequently, the generator J becomes

$$J = \begin{pmatrix} 0 & 0 & 0 & 0 \\ 0 & 0 & 0 & -1 \\ 1 & 0 & 0 & 0 \\ 0 & 0 & 0 & 0 \end{pmatrix}. \quad (\text{A9})$$

Thus, the symplectic matrix corresponding to the generator J is

$$S = \exp(J) = \begin{pmatrix} 1 & 0 & 0 & 0 \\ 0 & 1 & 0 & -1 \\ 1 & 0 & 1 & 0 \\ 0 & 0 & 0 & 1 \end{pmatrix}, \quad (\text{A10})$$

which is the same as the symplectic transformation matrix obtained using the BCH formula in the previous section.

APPENDIX B: FINAL STATE IN ARTHURS-KELLY MEASUREMENT SCHEME

The displacement vector and the covariance matrix of the transformed joint system-meters state are given by

$$\bar{\xi}' = \begin{pmatrix} \langle \hat{q} \rangle = q_0 \\ \langle \hat{p} \rangle = p_0 \\ \langle \hat{Q}_1 \rangle = q_0 \\ \langle \hat{P}_1 \rangle = 0 \\ \langle \hat{Q}_2 \rangle = 0 \\ \langle \hat{P}_2 \rangle = p_0 \end{pmatrix} \quad (\text{B1})$$

and

$$V' = \begin{pmatrix} \begin{array}{cc|cc|cc} \text{System} & & \text{Meter 1} & & \text{Meter 2} & \\ \hline & q & p & Q_1 & P_1 & Q_2 & P_2 \\ \hline (\Delta q)^2 + (\Delta Q_2)^2 & 0 & (\Delta q)^2 + \frac{(\Delta Q_2)^2}{2} & 0 & -(\Delta Q_2)^2 & 0 \\ 0 & (\Delta p)^2 + (\Delta P_1)^2 & 0 & -(\Delta P_1)^2 & 0 & (\Delta p)^2 + \frac{(\Delta P_1)^2}{2} \\ (\Delta q)^2 + \frac{(\Delta Q_2)^2}{2} & 0 & (\Delta q)^2 + (\Delta Q_1)^2 + \frac{(\Delta Q_2)^2}{4} & 0 & -\frac{(\Delta Q_2)^2}{2} & 0 \\ 0 & -(\Delta P_1)^2 & 0 & (\Delta P_1)^2 & 0 & -\frac{(\Delta P_1)^2}{2} \\ -(\Delta Q_2)^2 & 0 & -\frac{(\Delta Q_2)^2}{2} & 0 & (\Delta Q_2)^2 & 0 \\ 0 & (\Delta p)^2 + \frac{(\Delta P_1)^2}{2} & 0 & -\frac{(\Delta P_1)^2}{2} & 0 & (\Delta p)^2 + \frac{(\Delta P_1)^2}{4} + (\Delta P_2)^2 \end{array} \end{pmatrix}. \quad (\text{B2})$$

- [1] D. F. V. James, P. G. Kwiat, W. J. Munro, and A. G. White, *Phys. Rev. A* **64**, 052312 (2001).
- [2] M. Paris and J. Řeháček, editors, *Quantum State Estimation*, Lecture Notes in Physics, Vol. 649 (Springer-Verlag, Berlin, 2004).
- [3] A. I. Lvovsky and M. G. Raymer, *Rev. Mod. Phys.* **81**, 299 (2009).
- [4] G. Vallone and D. Dequal, *Phys. Rev. Lett.* **116**, 040502 (2016).
- [5] L. Calderaro, G. Foletto, D. Dequal, P. Villoresi, and G. Vallone, *Phys. Rev. Lett.* **121**, 230501 (2018).
- [6] G. S. Thekkadath, D. S. Phillips, J. F. F. Bulmer, W. R. Clements, A. Eckstein, B. A. Bell, J. Lugani, T. A. W. Wolterink, A. Lita, S. W. Nam *et al.*, *Phys. Rev. A* **101**, 031801(R) (2020).
- [7] H. P. Yuen and V. W. S. Chan, *Opt. Lett.* **8**, 177 (1983).
- [8] G. L. Abbas, V. W. S. Chan, and T. K. Yee, *Opt. Lett.* **8**, 419 (1983).
- [9] B. L. Schumaker, *Opt. Lett.* **9**, 189 (1984).
- [10] K. Banaszek and K. Wódkiewicz, *Phys. Rev. A* **55**, 3117 (1997).
- [11] K. Vogel and H. Risken, *Phys. Rev. A* **40**, 2847 (1989).
- [12] D. T. Smithey, M. Beck, M. G. Raymer, and A. Faridani, *Phys. Rev. Lett.* **70**, 1244 (1993).
- [13] J. Kiukas, P. Lahti, and J. Schultz, *Phys. Rev. A* **79**, 052119 (2009).
- [14] A. Di Lorenzo, *Phys. Rev. Lett.* **110**, 010404 (2013).
- [15] D. Das and Arvind, *J. Phys. A: Math. Theor.* **50**, 145307 (2017).
- [16] E. Arthurs Jr. and J. L. Kelly Jr., *Bell Syst. Tech. J.* **44**, 725 (1965).
- [17] A. Javan, E. A. Ballik, and W. L. Bond, *J. Opt. Soc. Am.* **52**, 96 (1962).
- [18] W. S. Read and R. G. Turner, *Appl. Opt.* **4**, 1570 (1965).
- [19] H. R. Carleton and W. T. Maloney, *Appl. Opt.* **7**, 1241 (1968).
- [20] H. Gerhardt, H. Welling, and A. Güttner, *Z. Phys.* **253**, 113 (1972).
- [21] H. Yuen and J. Shapiro, *IEEE Trans. Inf. Theory* **26**, 78 (1980).
- [22] H. P. Yuen, *Phys. Lett. A* **91**, 101 (1982).
- [23] E. Arthurs and M. S. Goodman, *Phys. Rev. Lett.* **60**, 2447 (1988).
- [24] J. Shapiro and S. Wagner, *IEEE J. Quantum Electron.* **20**, 803 (1984).
- [25] J. Shapiro, *IEEE J. Quantum Electron.* **21**, 237 (1985).
- [26] M. Collett, R. Loudon, and C. Gardiner, *J. Mod. Opt.* **34**, 881 (1987).
- [27] H. Martens and W. M. de Muynck, *Phys. Lett. A* **157**, 441 (1991).
- [28] M. G. Raymer, *Am. J. Phys.* **62**, 986 (1994).
- [29] J. Řeháček, Y. S. Teo, Z. Hradil, and S. Wallentowitz, *Sci. Rep.* **5**, 12289 (2015).
- [30] C. R. Müller, C. Peuntinger, T. Dirmeier, I. Khan, U. Vogl, C. Marquardt, G. Leuchs, L. L. Sánchez-Soto, Y. S. Teo, Z. Hradil, and J. Řeháček, *Phys. Rev. Lett.* **117**, 070801 (2016).
- [31] Y. S. Teo, C. R. Müller, H. Jeong, Z. Hradil, J. Řeháček, and L. L. Sánchez-Soto, *Phys. Rev. A* **95**, 042322 (2017).
- [32] S. Wallentowitz and W. Vogel, *Phys. Rev. A* **53**, 4528 (1996).
- [33] Y. S. Teo, H. Jeong, and L. L. Sánchez-Soto, *Phys. Rev. A* **96**, 042333 (2017).
- [34] M. Hillery, *Phys. Rev. A* **61**, 022309 (2000).
- [35] N. J. Cerf, M. Lévy, and G. Van Assche, *Phys. Rev. A* **63**, 052311 (2001).
- [36] F. Grosshans and P. Grangier, *Phys. Rev. Lett.* **88**, 057902 (2002).
- [37] P. Busch, *Int. J. Theor. Phys.* **24**, 63 (1985).
- [38] T. J. Bullock and P. Busch, *Phys. Rev. Lett.* **113**, 120401 (2014).
- [39] Arvind, S. Chaturvedi, and N. Mukunda, *Phys. Lett. A* **384**, 126543 (2020).
- [40] S. L. Braunstein and P. van Loock, *Rev. Mod. Phys.* **77**, 513 (2005).
- [41] C. Weedbrook, S. Pirandola, R. García-Patrón, N. J. Cerf, T. C. Ralph, J. H. Shapiro, and S. Lloyd, *Rev. Mod. Phys.* **84**, 621 (2012).
- [42] U. L. Andersen, M. Sabuncu, R. Filip, and G. Leuchs, *Phys. Rev. Lett.* **96**, 020409 (2006).
- [43] M. Sabuncu, L. Mišta, J. Fiurášek, R. Filip, G. Leuchs, and U. L. Andersen, *Phys. Rev. A* **76**, 032309 (2007).
- [44] M. Sabuncu, R. Filip, G. Leuchs, and U. L. Andersen, *Phys. Rev. A* **81**, 012325 (2010).
- [45] Arvind, B. Dutta, N. Mukunda, and R. Simon, *Pramana* **45**, 471 (1995).
- [46] G. Adesso, S. Ragy, and A. R. Lee, *Open Syst. Inf. Dyn.* **21**, 1440001 (2014).
- [47] E. Wigner, *Phys. Rev.* **40**, 749 (1932).
- [48] S. Olivares, *Eur. Phys. J.: Spec. Top.* **203**, 3 (2012).
- [49] R. Simon, *Phys. Rev. Lett.* **84**, 2726 (2000).
- [50] U. L. Andersen, R. Filip, J. Fiurášek, V. Josse, and G. Leuchs, *Phys. Rev. A* **72**, 060301(R) (2005).
- [51] M. Lassen, L. S. Madsen, M. Sabuncu, R. Filip, and U. L. Andersen, *Phys. Rev. A* **82**, 021801(R) (2010).